REMUNOM
ISSN 2178-6925

Received: 10/11/2026 - **Accepted:** 15/11/2026
Vol: 13.24
DOI: 10.66104/x7btvw60
Pages: 1-29

DISPERSÃO QUÍMICA E RECUPERAÇÃO MÁSSICA DO PRODUTO NÃO MAGNÉTICO NA SEPARAÇÃO DE BAUXITA

CHEMICAL DISPERSION AND MASS RECOVERY OF THE NONMAGNETIC PRODUCT IN BAUXITE SEPARATION

DISPERSIÓN QUÍMICA Y RECUPERACIÓN MÁSICA DEL PRODUCTO NO MAGNÉTICO EN LA SEPARACIÓN DE BAUXITA

Gabriel Mateus Oliveira Cubi
Mestre em Engenharia Química, Universidade Federal de Alfenas, Brazil
E-mail: gabriel.cubi@sou.unifal-mg.edu.br

Kaio Vinícius de Oliveira
Graduando em Engenharia de Minas, Universidade Federal de Alfenas, Brazil
E-mail: kaio.oliveira@unifal-mg.edu.br

Guilherme José Oliveira Cubi
Doutor em Tecnologia Mineral, Universidade Federal de Alfenas, Brazil
E-mail: guilherme.oliveira@unifal-mg.edu.br

Resumo

O condicionamento químico pode alterar as associações entre partículas em suspensões de bauxita e, consequentemente, afetar a distribuição de massa durante a separação magnética. Este estudo investigou o hexametafosfato de sódio (SHMP), o metassilicato de sódio (SMT) e o silicato de sódio (SS), por meio de caracterização mineralógica e granulométrica, medições de potencial zeta, ensaios de dispersão e recuperação mássica não magnética em densidades de fluxo magnético de 0,2 a 1,2 T. As fases identificadas foram gibbsita, caulinita, goethita, hematita e anatásio. O potencial zeta diminuiu de +20,2 mV em pH 2 para −42,9 mV em pH 12, com uma região próxima de zero entre pH 8 e 9. O grau de dispersão aumentou de 18% sem reagente para 46%, 41% e 38% com 3000 g/t de SHMP, SMT e SS, respectivamente. Entretanto, a classificação dos reagentes quanto à dispersão

CC BY

REMUNOM
ISSN 2178-6925

Received: 10/11/2026 - **Accepted:** 15/11/2026
Vol: 13.24
DOI: 10.66104/x7btvw60
Pages: 1-29

não previu consistentemente a recuperação mássica não magnética. Em 0,6 T, 600 g/t de SHMP proporcionaram recuperação de 90,8%, enquanto SMT e SS, na mesma dosagem, produziram 87,6% e 89,0%. Em 1,2 T, a maior recuperação apresentada foi de 79,8% com 2400 g/t de SMT, comparada com 70,4% no controle; o SS convergiu para 75,1% nas três dosagens. Os resultados indicam que a dispersão química e a captura magnética respondem conjuntamente à dosagem, às associações minerais e às condições de campo. Os dados demonstram alterações no rendimento mássico não magnético, enquanto análises químicas dos produtos permanecem necessárias para determinar a recuperação de alumina e a rejeição de ferro.

Palavras-chave: Bauxita; dispersão química; hexametafosfato de sódio; silicatos de sódio; separação magnética; recuperação mássica não magnética.

Abstract

Chemical conditioning can alter particle associations in bauxite suspensions and consequently affect mass partitioning during magnetic separation. This study investigated sodium hexametaphosphate (SHMP), sodium metasilicate (SMT), and sodium silicate (SS) using mineralogical and particle size characterization, zeta potential measurements, dispersion tests, and nonmagnetic mass recovery at magnetic flux densities from 0.2 to 1.2 T. The identified phases were gibbsite, kaolinite, goethite, hematite, and anatase. The zeta potential decreased from +20.2 mV at pH 2 to −42.9 mV at pH 12, with a near-zero region at pH 8 to 9. The degree of dispersion increased from 18% without reagent to 46%, 41%, and 38% at 3000 g/t of SHMP, SMT, and SS, respectively. However, the reagent ranking for dispersion did not consistently predict nonmagnetic mass recovery. At 0.6 T, 600 g/t SHMP produced 90.8% recovery, whereas SMT and SS at the same dosage produced 87.6% and 89.0%. At 1.2 T, the highest reported recovery was 79.8% with 2400 g/t SMT, compared with 70.4% for the control; SS converged to 75.1% across the three dosages. These results indicate that chemical dispersion and magnetic capture respond jointly to reagent dosage, mineral associations, and field conditions. The findings establish changes in nonmagnetic mass yield, while product assays remain necessary to determine alumina recovery and iron rejection.

Keywords: Bauxite; chemical dispersion; sodium hexametaphosphate; sodium silicates; magnetic separation; nonmagnetic mass recovery.

Resumen

El acondicionamiento químico puede alterar las asociaciones entre partículas en suspensiones de bauxita y, por consiguiente, afectar la distribución de masa durante la separación magnética. Este estudio investigó el hexametafosfato de sodio (SHMP), el metasilicato de sodio (SMT) y el silicato de sodio (SS), mediante caracterización mineralógica y granulométrica, mediciones de potencial zeta, ensayos de dispersión y recuperación másica no magnética con densidades de flujo magnético de 0,2 a 1,2 T. Las fases identificadas fueron gibbsita, caolinita, goethita, hematita y anatasa. El potencial

CC BY

REMUNOM
ISSN 2178-6925

Received: 10/11/2026 - **Accepted:** 15/11/2026
Vol: 13.24
DOI: 10.66104/x7btvw60
Pages: 1-29

zeta disminuyó de +20,2 mV a pH 2 a −42,9 mV a pH 12, con una región cercana a cero entre pH 8 y 9. El grado de dispersión aumentó del 18% sin reactivo al 46%, 41% y 38% con 3000 g/t de SHMP, SMT y SS, respectivamente. Sin embargo, la clasificación de los reactivos según la dispersión no predijo consistentemente la recuperación másica no magnética. A 0,6 T, 600 g/t de SHMP proporcionaron una recuperación del 90,8%, mientras que SMT y SS, con la misma dosificación, produjeron el 87,6% y el 89,0%. A 1,2 T, la mayor recuperación presentada fue del 79,8% con 2400 g/t de SMT, frente al 70,4% del control; el SS convergió al 75,1% en las tres dosificaciones. Los resultados indican que la dispersión química y la captura magnética responden conjuntamente a la dosificación, las asociaciones minerales y las condiciones de campo. Los datos demuestran cambios en el rendimiento másico no magnético, mientras que los análisis químicos de los productos siguen siendo necesarios para determinar la recuperación de alúmina y el rechazo de hierro.
Palabras clave: Bauxita; dispersión química; hexametafosfato de sodio; silicatos de sodio; separación magnética; recuperación másica no magnética.

1. Introduction

Bauxite beneficiation must address the association of aluminum-bearing minerals with iron oxides, titanium minerals, and silicate gangue. In gibbsitic materials, kaolinite is particularly relevant because its removal involves separating two aluminum-containing phases with different implications for alumina production. Iron-bearing phases introduce a further separation problem: their response to magnetic forces depends on mineral identity, particle size, and association with the aluminum minerals. Consequently, identifying gibbsite in an ore does not by itself establish the recoverable alumina fraction or the suitability of a particular beneficiation route (Rodrigues et al.; D. S. Rao and Das).

Magnetic separation has long been investigated for ferruginous bauxite. Bolsaitis and colleagues examined high-gradient magnetic separation as a means of increasing gibbsite concentration. Kasai and colleagues subsequently demonstrated that grinding, alkaline conditioning, or dispersant addition could affect the treatment of an Indonesian bauxite containing goethite and hematite. These studies establish that magnetic response cannot be understood exclusively through the applied field: the physical and chemical state of the feed also matters. The challenge is especially pronounced when particles of different minerals remain

CC BY

REMUNOM
ISSN 2178-6925

Received: 10/11/2026 - **Accepted:** 15/11/2026
Vol: 13.24
DOI: 10.66104/x7btvw60
Pages: 1-29

attached through surface interactions after mechanical liberation.

The relevance of this problem is evident in Brazilian bauxite circuits. Kurusu and colleagues described magnetic separation of a flotation product containing aluminum, iron, and titanium minerals, showing why flotation and magnetic separation can perform complementary roles. A more recent investigation by Ashrafi and colleagues found that high-gradient magnetic separation and flotation did not sufficiently remove impurities from a low-grade bauxite with fine mineral dissemination. These contrasting outcomes show that successful processing depends on the nature of the mineral associations, not simply on the presence of an equipment stage capable of separating pure minerals.

Particle association can occur at two distinct levels. Minerals may form locked particles that require comminution for liberation, or liberated particles may associate through electrostatic attraction, van der Waals forces, and other interfacial interactions. Chemical dispersants primarily address the latter level. They may reduce heteroaggregation between iron-bearing and aluminum-bearing particles, prevent clay coatings, and modify the flow of particles through a separator. They cannot be assumed to liberate mineral inclusions inside coherent grains. This distinction is necessary when interpreting an increased nonmagnetic mass yield after reagent addition.

Surface chemistry provides a basis for understanding these effects. The balance between attractive and repulsive interparticle forces changes with pH, ionic composition, and adsorbed species, affecting both aggregation and suspension rheology (Johnson et al.). For kaolinite, a single uniformly charged surface is an inadequate representation: its silica-like and alumina-like faces have distinct charging characteristics, and edges provide additional reactive sites. Experimental investigations of surface charge and electrokinetic behavior document this heterogeneity (Herrington et al.; Williams and Williams; Miller et al.). Atomic force microscopy has also resolved different pH-dependent charging responses on the two basal planes (Kumar et al.). In a multiphase bauxite, these contrasts operate between mineral species as well as within individual clay particles.

Zeta potential offers a useful indicator of electrokinetic behavior, but its

CC BY

REMUNOM
ISSN 2178-6925

Received: 10/11/2026 - **Accepted:** 15/11/2026
Vol: 13.24
DOI: 10.66104/x7btvw60
Pages: 1-29

interpretation requires attention to the solution and to the particle population being measured. Alkan and colleagues showed that multivalent electrolytes can alter or reverse kaolinite electrokinetic charge. Models based on electrical double-layer repulsion and van der Waals attraction therefore provide a useful starting point, although clay anisotropy and charge heterogeneity complicate quantitative predictions (Missana and Adell). A bulk zeta potential close to zero does not mean that every mineral surface is uncharged, and a negative bulk value does not exclude local attractive contacts.

Inorganic dispersants can modify this interfacial balance through adsorption and interactions with dissolved ions. Sodium hexametaphosphate has been investigated through adsorption thermodynamics on kaolinite and atomistic calculations involving its aluminol surface (Castellini et al., “Thermodynamic Aspects”; Han et al.). Silicate reagents also interact with mineral surfaces, but their aqueous species depend on solution composition and concentration (Bass and Turner). Studies on kaolinite and hematite show that sodium silicate and sodium metasilicate cannot be treated as interchangeable additives with a universal response (Ma; Quezada et al.). Their practical comparison must consider both measured dispersion and the behavior of the subsequent separation operation.

Evidence from bauxite suspensions reinforces this requirement. Gonçalves and colleagues reported viscosity reduction with chemical additives in a very fine bauxite tailing. Batista e Silva and colleagues related improved bauxite flotation to particle dispersion and reduced kaolinite coating under chemical and ultrasonic conditioning. These observations establish the relevance of particle associations, but neither rheological improvement nor flotation response directly predicts nonmagnetic yield. A magnetic separator exposes the conditioned suspension to a different balance of capture, drag, and particle interactions.

There is also a fundamental ambiguity in the desired direction of dispersion. Breaking mixed aggregates may release gibbsite into the nonmagnetic stream, increasing its mass yield. Dispersing aggregates of weakly magnetic fines may also reduce their effective capture and increase the same yield through retention of iron-bearing material in that stream. Conversely, removal of coatings may improve

CC BY

REMUNOM
ISSN 2178-6925

Received: 10/11/2026 - **Accepted:** 15/11/2026
Vol: 13.24
DOI: 10.66104/x7btvw60
Pages: 1-29

capture of liberated iron minerals and decrease nonmagnetic yield. A bulk dispersion measurement cannot distinguish these alternatives. Investigations of single-mineral dispersion and selective flocculation before magnetic separation illustrate why the mineral distribution within aggregates must be considered (Wang and Heiskanen; Alvim and Fernandes Lima).

The present study evaluates the influence of SHMP, SMT, and SS on bauxite dispersion and nonmagnetic mass recovery over a range of reagent dosages and magnetic flux densities. Mineralogical, particle size, and electrokinetic characterization are used to interpret the measured responses. The central objective is to establish whether the ranking obtained from dispersion tests is retained during magnetic separation and how that relationship changes with field and dosage. The contribution is a comparative assessment of chemical conditioning and mass partitioning, with a clear distinction between nonmagnetic yield and product quality.

2. Materials and Methds

2.1 Bauxite characterization

The bauxite originated from Minas Gerais, Brazil, and was received as a previously sampled material. Details regarding the original sampling procedure and the representativeness of the collected material were not available. It was oven-dried at 80 °C to constant mass and homogenized using an elongated pile. Mineralogical characterization was performed using a Bruker D8 Discover diffractometer with Cu Kα radiation (λ = 1.5406 Å). Diffraction patterns were collected over a 2θ range of 5° to 70°, with a step size of 0.02°. The principal reflections were used for qualitative phase identification; peak intensities were not converted into mineral mass fractions.

Particle size distribution was determined by wet sieving using sieve apertures of 300, 212, 150, 106, 75, 53, and 38 μm. Results were expressed as cumulative mass passing percentage and plotted against sieve aperture on a logarithmic scale (Figure 1b).

CC BY

REMUNOM
ISSN 2178-6925

Received: 10/11/2026 - **Accepted:** 15/11/2026
Vol: 13.24
DOI: 10.66104/x7btvw60
Pages: 1-29

2.2 Zeta potential measurements

Zeta potential was measured using a Zetasizer Nano ZS instrument (Malvern Instruments). For each measurement, 0.05 g of the homogenized bauxite sample was dispersed in 50 mL of distilled water, without prior particle-size classification. The pH was adjusted with HCl and NaOH solutions over the range from 2 to 12, in increments of one pH unit. Zeta potential was expressed in millivolts and evaluated in terms of its sign, magnitude, and transition through zero. The near-zero interval was used to identify the apparent isoelectric region of the suspension, rather than the point of zero surface charge of an individual mineral. Figure 2 represents the baseline pH series without dispersant addition.

2.3 Chemical dispersants and dispersion tests

The evaluated dispersants were analytical-grade sodium hexametaphosphate (SHMP), sodium metasilicate pentahydrate ($Na_2SiO_3 \cdot 5H_2O$; SMT), and sodium silicate (SS), all in solid state. All reagents used in the study were analytical grade. The dispersion series comprised a reagent-free control and dosages of 100, 200, 400, 600, 800, 1000, 1200, 1500, 2000, and 3000 g/t, expressed per unit dry mass of bauxite. All tests were conducted using water from the same source, without pH adjustment during dispersant conditioning.

The degree of dispersion was determined using a sedimentation procedure. For each test, 5 g of bauxite was suspended in 100 mL of distilled water and stirred for 1 min. After dispersant addition, the suspension was conditioned for an additional 2 min and then allowed to settle for 1 min. After settling, the upper 50 mL of the suspension was carefully withdrawn using a syringe, avoiding disturbance of the settled material. The withdrawn supernatant was transferred directly to an oven, without prior filtration, and the dried residue was weighed. No correction for dissolved reagent residues was applied. At the highest dosage (3000 g/t), the total dispersant mass added was 15 mg, corresponding to 0.3% of the initial sample

CC BY

REMUNOM
ISSN 2178-6925

Received: 10/11/2026 - **Accepted:** 15/11/2026
Vol: 13.24
DOI: 10.66104/x7btvw60
Pages: 1-29

mass. Even if entirely retained in the withdrawn fraction, this amount would contribute at most 0.3 percentage point to the measured dispersion index.

The degree of dispersion was calculated as DD (%) = 100 m_s/m_0, where m_s is the dry solids mass recovered from the withdrawn supernatant and m_0 is the initial dry sample mass (5 g). No volume correction was applied; therefore, DD represents the percentage of the initial sample mass recovered in the withdrawn aliquot.

All dispersion tests were performed in triplicate, and the results are expressed as mean values with error bars representing one standard deviation.

2.4 Magnetic separation experiments

Magnetic separation compared the reagent-free control with 600, 1200, and 2400 g/t of each dispersant. The tested nonzero field values were 0.2, 0.4, 0.6, 0.8, 1.0, and 1.2 T.

Wet high-intensity magnetic separation was performed using an Inbras L4-20 separator equipped with a 1.5 mm matrix. Before separation, the pulp was conditioned with the dispersant for 2 min. The magnetic flux density was adjusted directly through the equipment controls, and the pulp was fed at a constant rate. Each pulp was prepared with 100 g of dry bauxite and 400 mL of tap water, corresponding to approximately 20% solids by mass. The starting water pH was near 6, and pH was measured after reagent addition. The pulp was fed to the separator at a constant rate. The cleaning-water volume was 200 mL (while magnetic field was still on), and the washing-water volume was 800 mL per test.

Magnetic separation was performed sequentially, with the magnetic flux density progressively increased from 0.2 to 1.2 T. At each stage, the retained magnetic fraction was collected, dried, and weighed, while the nonmagnetic fraction was used as feed for the subsequent stage. Nonmagnetic mass recovery was calculated by subtracting the cumulative dry mass of the magnetic products from the initial feed mass (100 g), expressing the remaining mass as a percentage of the initial mass.

All magnetic separation tests were performed in triplicate, and the results are

CC BY

REMUNOM
ISSN 2178-6925

Received: 10/11/2026 - **Accepted:** 15/11/2026
Vol: 13.24
DOI: 10.66104/x7btvw60
Pages: 1-29

expressed as mean values with error bars representing one standard deviation.

3. Results and Discussion

3.1 Characterization

Figure 1a identifies gibbsite, kaolinite, goethite, hematite, and anatase. The strongest reflection is assigned to gibbsite near 18° in 2θ, accompanied by additional gibbsite reflections. Kaolinite is identified by reflections near 12° and 25°, while the iron-bearing phases contribute features in overlapping portions of the pattern. This assemblage provides a coherent mineralogical basis for evaluating dispersion before magnetic separation: aluminum hydroxide, an aluminosilicate clay, and iron oxides or oxyhydroxides coexist in the feed. The intense gibbsite peak confirms a strong crystalline signature, but does not establish its weight fraction.

The assemblage resembles the broad mineral groups reported in other bauxites while retaining important distinctions. D. S. Rao and Das identified gibbsite, boehmite, iron-bearing minerals, silicates, and titanium phases in an Indian material, with impurities also occurring as inclusions within aluminum-bearing particles. In the present pattern, boehmite is not among the assigned phases. The comparison supports attention to mineral associations, but does not establish that the present bauxite contains the same inclusion textures. Diffraction identifies phases without resolving whether they occur as liberated grains, coatings, or locked composites.

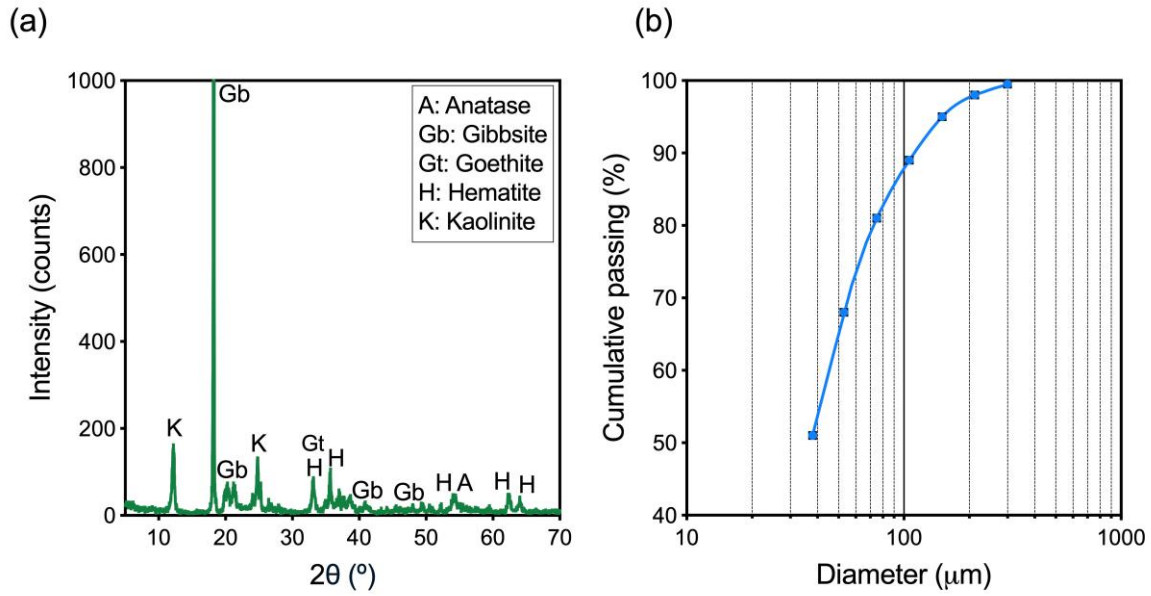
Hematite and goethite provide a plausible basis for magnetic capture, but their responses should not be considered identical. Shao and colleagues found markedly different magnetic separation behavior among iron mineral samples, including differences between two hematites and limited recovery of weakly paramagnetic goethite and limonite under their conditions. Accordingly, the amount of material captured from the present bauxite cannot be equated to the amount of iron-bearing phases present. Anatase identification also does not establish its partitioning: association with other grains may be more influential than the response of an isolated anatase particle.

CC BY

REMUNOM
ISSN 2178-6925

Received: 10/11/2026 - **Accepted:** 15/11/2026
Vol: 13.24
DOI: 10.66104/x7btvw60
Pages: 1-29

Figure 1. Mineralogical and particle size characterization of the bauxite: (a) X-ray diffraction pattern with the assigned phases anatase (A), gibbsite (Gb), goethite (Gt), hematite (H), and kaolinite (K); (b) cumulative mass passing distribution determined by wet sieving, with sieve aperture in micrometers on a logarithmic axis.



The cumulative size distribution in Figure 1b contains points near 38, 53, 75, 106, 150, 212, and 300 μm, with passing percentages of 51%, 68%, 81%, 89%, 95%, 98%, and 99.5%, respectively. Interpolation gives d_{80} of 73 μm and d_{90} of 112 μm. The first displayed point already exceeds 50% passing; therefore, d_{50} lies below 38 μm and cannot be assigned an exact value without extrapolating beyond the measured points shown. The same limitation prevents determination of d_{10}.

Approximately half of the cumulative distribution lies below the smallest displayed diameter, while most of the remainder is contained below 150 μm. The figure therefore indicates a substantial fine fraction but does not quantify the ultrafine fraction. These particles can contribute disproportionately to surface-mediated interactions. A small amount of high-area clay may coat larger particles or bridge different mineral populations without contributing a corresponding fraction of total mass. The cumulative curve alone cannot identify which mineral occupies each size interval, and cannot separate individual fine particles from aggregates surviving the sizing preparation.

CC BY

REMUNOM
ISSN 2178-6925

Received: 10/11/2026 - **Accepted:** 15/11/2026
Vol: 13.24
DOI: 10.66104/x7btvw60
Pages: 1-29

The coupling of size and texture is consequential for beneficiation. Ashrafi and colleagues reported only 31.15% iron oxide removal at 1.8 T from a low-grade bauxite, attributing the limited performance to fine dissemination. The present study reaches a lower maximum field, but this does not permit prediction of a lower or higher iron rejection because liberation and product assays are unavailable. Chemical conditioning may change contacts among liberated particles; it cannot be assumed to overcome the textural limitations responsible for poor separation in another ore.

3.2 Electrokinetic behavior of bauxite particles

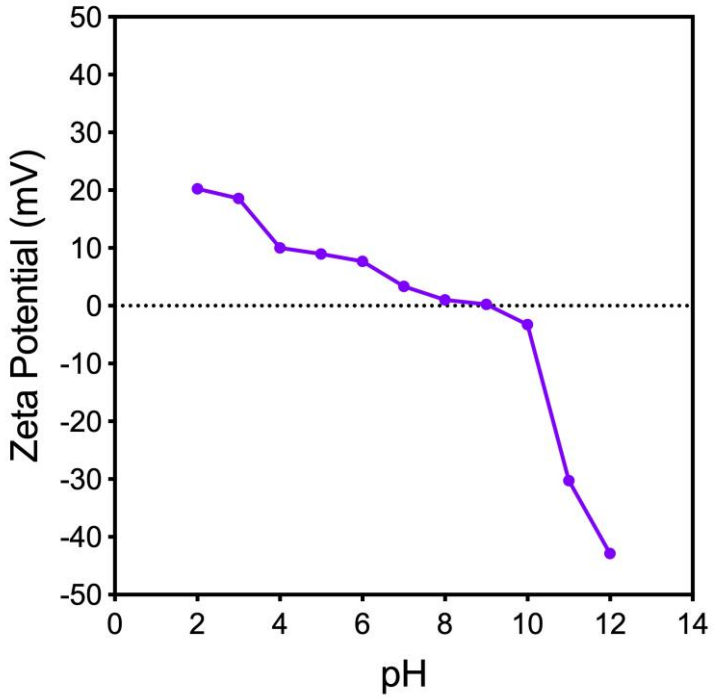
The zeta potential decreases systematically with pH (Figure 2). Values are +20.2 and +18.5 mV at pH 2 and 3, followed by +10.0, +9.0, and +7.6 mV at pH 4, 5, and 6. The potential approaches zero through +3.4 mV at pH 7, +1.0 mV at pH 8, and +0.2 mV at pH 9. It becomes −3.3 mV at pH 10, then decreases sharply to −30.3 mV at pH 11 and −42.9 mV at pH 12. The sign change occurs between pH 9 and 10, with the pH 8 to 9 interval already exhibiting very small potential magnitudes.

CC BY

REMUNOM
ISSN 2178-6925

Received: 10/11/2026 - **Accepted:** 15/11/2026
Vol: 13.24
DOI: 10.66104/x7btvw60
Pages: 1-29

Figure 2. Figure 2. Zeta potential of the bauxite suspension as a function of pH from 2 to 12. The dotted horizontal line marks zero potential.



The positive values under acidic conditions are consistent with protonated hydroxylated surfaces, whereas the negative alkaline response is consistent with increasing deprotonation. These reactions can be represented conceptually as proton uptake by surface hydroxyl groups and proton release from those groups as alkalinity increases. However, the curve does not resolve separate contributions from gibbsite, goethite, hematite, or kaolinite. It also does not establish that the steep change between pH 10 and 11 is caused by a single surface reaction. Ion release, adsorption, and changes in the measured dispersed population could contribute.

The apparent isoelectric region differs substantially from that of some isolated kaolinites. Alkan and colleagues reported a kaolinite isoelectric point near pH 2.35, while also showing charge reversal in the presence of several multivalent cations. The present positive response extending toward pH 9 should therefore not be interpreted as intrinsic kaolinite behavior. Hydroxide-rich surfaces and solution chemistry can influence the composite response. Herrington and colleagues likewise distinguished more than one contribution to kaolin surface charge, reinforcing the need to avoid a single-site interpretation.

CC BY

REMUNOM
ISSN 2178-6925

Received: 10/11/2026 - **Accepted:** 15/11/2026
Vol: 13.24
DOI: 10.66104/x7btvw60
Pages: 1-29

Particle-level heterogeneity remains relevant even when the measured average is small. Kumar and colleagues found negatively charged silica-like kaolinite faces at pH 4 and above, whereas the gibbsite-like faces changed sign at higher pH. Their results illustrate how unlike surface regions can attract under conditions that do not appear strongly charged in a bulk measurement. In the bauxite suspension, analogous contrasts may operate between kaolinite and hydroxide-rich particles, permitting edge-to-face contacts, coating, or heteroaggregation. These are mechanistic possibilities, not direct observations of aggregate structure in the present sample.

The near-zero interval suggests limited electrostatic stabilization under the measurement conditions. The large negative magnitudes at pH 11 and 12 are consistent with a greater potential for repulsion, but do not prove a particular dispersion percentage or an optimum separation pH. Missana and Adell examined the limitations of applying conventional DLVO predictions to clays with structural and pH-dependent charge. Williams and Williams also showed that preparation and electrolyte conditions influence kaolinite electrophoretic measurements. Consequently, the baseline curve cannot substitute for measurements in the actual reagent-conditioned separation water.

At the nominal starting pH near 6 used for magnetic separation, the baseline potential is only +7.6 mV. This provides a plausible context for chemically induced changes in particle association. It does not establish the potential after adding SHMP, SMT, or SS, nor does it demonstrate that the reagents act exclusively through charge reversal.

3.3 Effect of dispersant type and dosage on the degree of dispersion

The three reagents increase the degree of dispersion over the reagent-free value of 18% (Figure 3). SHMP exhibited the highest observed dispersion index throughout the tested dosage range, followed numerically by SMT and SS.. At 600 g/t, the respective values are 33%, 29%, and 27%; at 1200 g/t they reach 41%, 36%, and 33%. At 3000 g/t, the values are 46%, 41%, and 38%, corresponding to gains

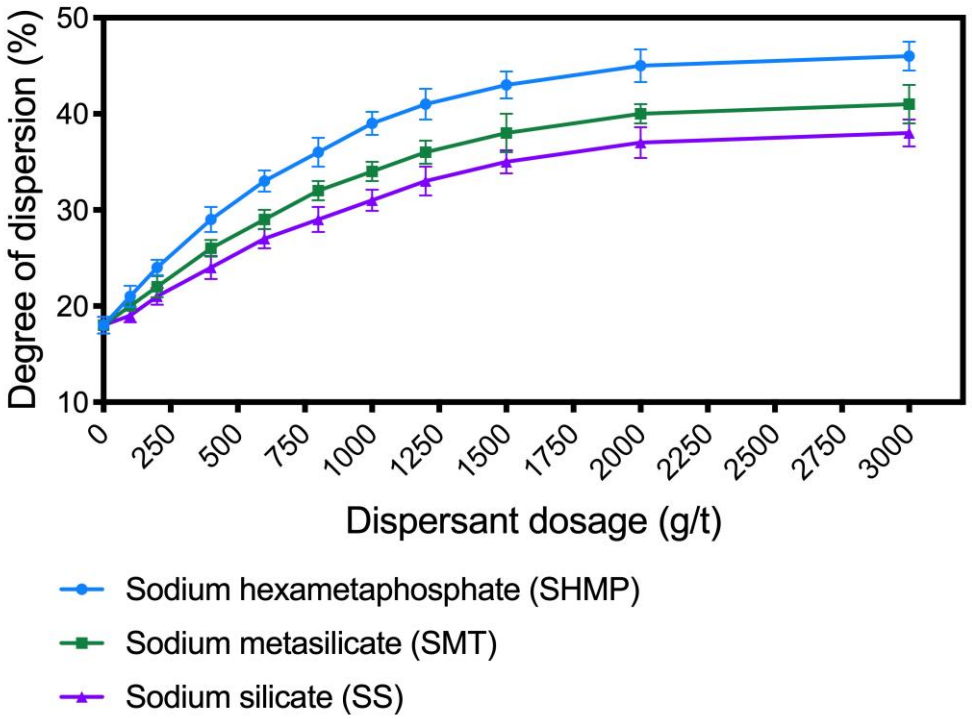
CC BY

REMUNOM
ISSN 2178-6925

Received: 10/11/2026 - **Accepted:** 15/11/2026
Vol: 13.24
DOI: 10.66104/x7btvw60
Pages: 1-29

of 28, 23, and 20 percentage points over the control. The reagent order is therefore consistent across a broad range of applied mass dosages.

Figure 3. Degree of dispersion of bauxite as a function of sodium hexametaphosphate (SHMP), sodium metasilicate (SMT), and sodium silicate (SS) dosage. The zero-dosage point is the reagent-free control. Error bars represent standard deviations (n = 3).



The dosage-response curves show diminishing incremental gains. Increasing SHMP from 600 to 1200 g/t adds 8 percentage points, whereas increasing it from 2000 to 3000 g/t adds only 1 point. The corresponding increments are 7 and 1 points for SMT, and 6 and 1 points for SS. Thus, the final 1000 g/t produces little additional dispersion for any reagent. This behavior indicates diminishing incremental gains in the operational dispersion index. Since only half of the initial suspension volume was withdrawn, the values should not be interpreted as the total fraction of dispersed solids. In a uniformly mixed suspension, the withdrawn volume would contain approximately half of the suspended mass. However, the actual recovery also depends on the particle concentration profile established during sedimentation.

SHMP also achieves dispersion levels at lower dosages than the silicates. A degree of dispersion of 41% is attained with 1200 g/t SHMP and 3000 g/t SMT, while

CC BY

REMUNOM
ISSN 2178-6925

Received: 10/11/2026 - **Accepted:** 15/11/2026
Vol: 13.24
DOI: 10.66104/x7btvw60
Pages: 1-29

SS remains below that value within the tested range. SHMP at 1000 g/t gives 39%, exceeding SS at 3000 g/t by 1 percentage point. These comparisons are useful for reagent screening, although they do not establish cost savings because reagent prices, active contents, and downstream consequences were not evaluated. They also represent mass-dosage comparisons, not equal molar concentrations of chemically equivalent species.

Adsorption on aluminum-containing surface sites provides a plausible explanation for the strong SHMP response. Castellini and colleagues investigated hexametaphosphate adsorption on kaolinite as a function of temperature and clay concentration (“Thermodynamic Aspects”). Han and colleagues used molecular simulations to examine interactions with the kaolinite alumina surface, supporting increased negative surface character after adsorption. In the present multiphase feed, such interactions could reduce attractive contacts involving clay surfaces. Complexation of dissolved cations is another possible contribution, but neither adsorption density nor solution speciation was measured here.

The importance of mineral-specific chemistry is illustrated by investigations extending beyond kaolinite. Castellini and colleagues examined different uptake and ion-release processes for SHMP interacting with illite and montmorillonite (“Sodium Hexametaphosphate Interaction”). Those mechanisms cannot be transferred directly to the present kaolinite-bearing bauxite because 2:1 clays possess different structural features. Their relevance is that “clay dispersion” is not a single universal response. Similarly, work using malachite green adsorption as a surface probe showed that phosphate and disilicate treatments modify kaolinite surface properties (“Deflocculant Effects”). These findings support a surface-conditioning interpretation without identifying a unique adsorption geometry in the present ore.

The SMT–SS difference may reflect alkalinity, silicate speciation, and differing affinity for the available surfaces. Bass and Turner showed that the distribution of aqueous silicate anions depends on concentration and the relative amounts of silica and cations. Andreola and colleagues further demonstrated that prior phosphate or disilicate treatment changes subsequent kaolinite deflocculation, while associated work linked these differences to ion release into solution (Andreola et al., “Role of

CC BY

REMUNOM
ISSN 2178-6925

Received: 10/11/2026 - **Accepted:** 15/11/2026
Vol: 13.24
DOI: 10.66104/x7btvw60
Pages: 1-29

the Surface Treatment"; Andreola et al., "Release of Ions"). Consequently, the 3 to 5 percentage-point advantage of SMT over SS at intermediate and high dosages cannot be attributed solely to nominal chemical names. The SS modulus and the use of pentahydrated SMT are relevant when comparing mass dosages with concentrations of dissolved silicate species.

Comparison with bauxite tailings also shows why the required dosage is sample dependent. Gonçalves and colleagues studied a material with d_{50} below 5 μm at 33.5% solids and reported viscosity reduction using 101.75 g/t SHMP. The present dispersion test requires larger dosages to approach its upper response, but it measures a different property in a different particle population. A viscosity decrease and an increase in suspended mass need not occur at the same dose. Amorós and colleagues explicitly investigated the coupled influence of silicate concentration and solids volume fraction on kaolin electrokinetics and rheology, emphasizing the importance of suspension conditions when comparing reagent demand.

3.4 Effect of dispersion on magnetic separation

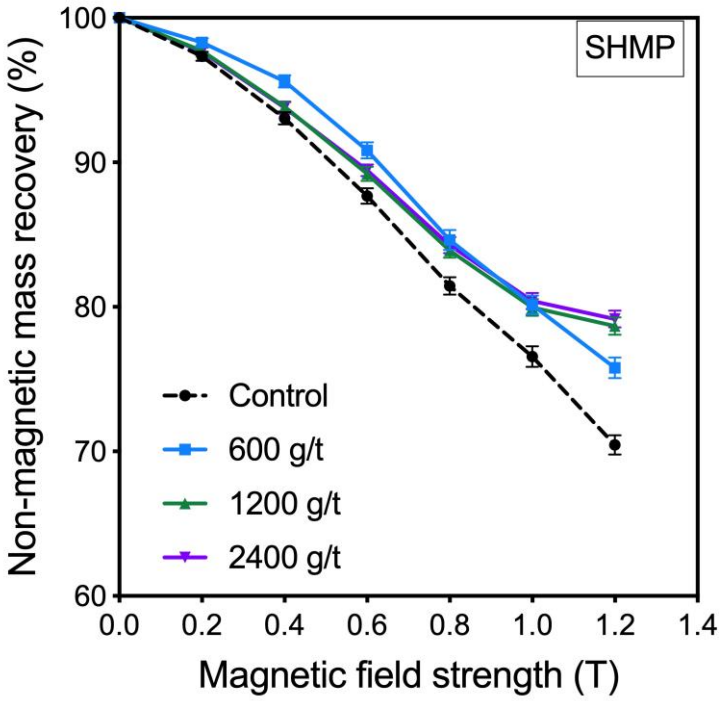
The control nonmagnetic recovery decreases from 97.3% at 0.2 T to 93.0% at 0.4 T, 87.7% at 0.6 T, 81.4% at 0.8 T, 76.5% at 1.0 T, and 70.4% at 1.2 T. SHMP modifies this decline in a field-dependent manner (Figure 4). At 600 g/t, recovery is 98.3% at 0.2 T, 95.6% at 0.4 T, and 90.8% at 0.6 T. The advantages over the control at these fields are 1.0, 2.6, and 3.1 percentage points. The same treatment gives 84.6% at 0.8 T and 75.8% at 1.2 T.

CC BY

REMUNOM
ISSN 2178-6925

Received: 10/11/2026 - **Accepted:** 15/11/2026
Vol: 13.24
DOI: 10.66104/x7btvw60
Pages: 1-29

Figure 4. Nonmagnetic mass recovery of bauxite versus magnetic flux density for the reagent-free control and sodium hexametaphosphate (SHMP) at 600, 1200, and 2400 g/t. Error bars represent standard deviations (n = 3).



The ordering among SHMP dosages changes at high field. At 0.6 T, 600 g/t produces 90.8%, compared with 89.2% and 89.5% at 1200 and 2400 g/t. At 1.2 T, these recoveries become 75.8%, 78.7%, and 79.2%, respectively. Thus, the lowest dosage performs better in terms of nonmagnetic mass yield at intermediate field, while the higher dosages retain more nonmagnetic mass at the maximum field. Increasing dosage does not therefore produce a uniformly positive yield response across the field range.

At 1.2 T, the gains over the control are 5.4, 8.3, and 8.8 percentage points for the three SHMP dosages. Doubling dosage from 1200 to 2400 g/t adds only 0.5 percentage point, a small descriptive difference in relation to the error bars. The clear response is the separation between the conditioned and control curves; the smaller difference between the two higher dosages does not establish a statistically superior operating condition. By contrast, their separation from the 600 g/t curve becomes visibly greater at the maximum field.

A possible explanation is that higher dosage better maintains particle

CC BY

REMUNOM
ISSN 2178-6925

Received: 10/11/2026 - **Accepted:** 15/11/2026
Vol: 13.24
DOI: 10.66104/x7btvw60
Pages: 1-29

separation under conditions of stronger magnetic capture and denser deposits within the collecting region. Reduced attachment of nonmagnetic particles to captured material would increase nonmagnetic yield. Another possibility is that SHMP disperses iron-bearing aggregates into smaller particles that are less efficiently collected. Liu and colleagues investigated SHMP-assisted separation of fine quartz from magnetite through dispersion and magnetic separation tests. That work provides an operational precedent, but magnetite is not identified in the present bauxite, so its capture response cannot be used as a quantitative model for the hematite–goethite assemblage.

Direct bauxite evidence provides a closer comparison. Kasai and colleagues obtained a nonmagnetic yield near 80%, with alumina increasing from about 51% to 56% and iron oxide decreasing from about 14% to 8%, after conditions involving liberation and chemical control were evaluated. The present SHMP yields at 1.2 T approach that mass-yield range, but similarity in yield does not establish similar composition. Their product assays supported an upgrading conclusion that cannot be inferred from the present recovery curves alone.

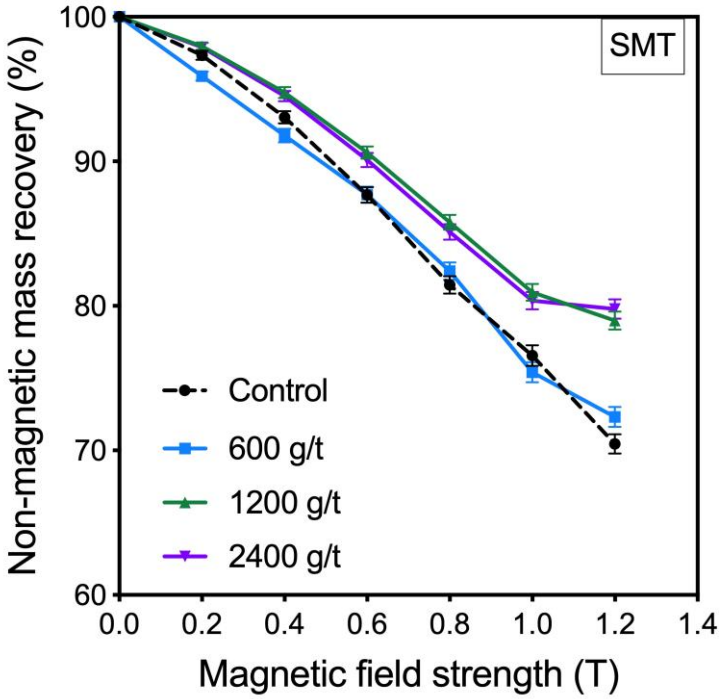
SMT shows a particularly clear distinction between the lowest dosage and the two higher dosages (Figure 5). At 0.4 T, nonmagnetic recovery is 91.8% with 600 g/t, below the 93.0% control. Increasing dosage to 1200 and 2400 g/t raises recovery to 94.8% and 94.5%. At 0.6 T, the lowest dosage gives 87.6%, effectively matching the 87.7% control at the resolution of the graph, while the higher dosages give 90.6% and 90.1%. A dispersant designation therefore does not imply an increase in nonmagnetic yield at every dosage and field.

CC BY

REMUNOM
ISSN 2178-6925

Received: 10/11/2026 - **Accepted:** 15/11/2026
Vol: 13.24
DOI: 10.66104/x7btvw60
Pages: 1-29

Figure 5. Nonmagnetic mass recovery of bauxite versus magnetic flux density for the reagent-free control and sodium metasilicate (SMT) at 600, 1200, and 2400 g/t. Error bars represent standard deviations (n = 3).



The dosage separation persists at high field. At 1.0 T, recovery is 75.4% with 600 g/t, compared with 80.9% and 80.4% at 1200 and 2400 g/t. At 1.2 T, the corresponding values are 72.3%, 79.0%, and 79.8%. Relative to the control, the maximum-field gains are 1.9, 8.6, and 9.4 percentage points. The last value corresponds to a 13.4% relative increase in nonmagnetic mass recovery, calculated from the 70.4% baseline. It is a relative change in mass yield, not an alumina-recovery improvement.

The intermediate dosage gives slightly higher recovery than 2400 g/t from 0.2 to 1.0 T, whereas the highest dosage leads at 1.2 T. This reversal is small compared with the large gap between 600 and 1200 g/t. At the maximum field, raising dosage from 600 to 1200 g/t adds 6.7 percentage points, while the next doubling adds 0.8 point. The stronger evidence therefore concerns the transition from low to intermediate dosage; the narrow ordering of the two upper curves remains descriptive.

CC BY

REMUNOM
ISSN 2178-6925

Received: 10/11/2026 - **Accepted:** 15/11/2026
Vol: 13.24
DOI: 10.66104/x7btvw60
Pages: 1-29

Quezada and colleagues combined rheological measurements with molecular simulations to investigate metasilicate–hematite interactions. They reported reduced yield stress, stable surface adsorption, and a role for sodium-mediated cation bridging in the simulated adsorption process. Such findings make modification of iron-oxide particle associations a plausible contributor here. However, the present recovery response does not determine whether SMT mainly releases gibbsite from mixed aggregates or reduces capture of dispersed iron-bearing fines. Both effects can raise the nonmagnetic mass fraction.

The comparison with SHMP is informative. At 600 g/t and 0.6 T, SHMP gives 90.8%, exceeding SMT by 3.2 percentage points. At 1200 g/t, SMT gives 90.6%, exceeding SHMP by 1.4 points at the same field. This is a reversal of the dispersion ranking, because SHMP remains the stronger dispersant in Figure 3. Haselhuhn found that calcium activation strongly influenced inorganic dispersant effectiveness in hematite-rich ore at pH 11. Although those conditions differ from the present study, the result demonstrates why reagent performance can depend on water–surface interactions rather than on reagent concentration alone.

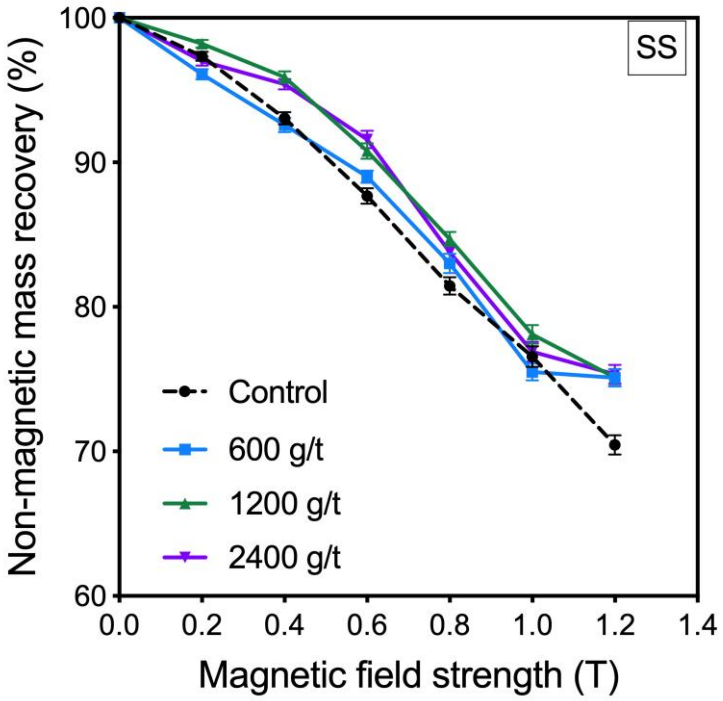
Finally, SS also produces a field-dependent response, but its most distinctive feature is convergence of the dosage curves at 1.2 T (Figure 6). At 0.4 T, recovery is 92.5% with 600 g/t, 95.9% with 1200 g/t, and 95.4% with 2400 g/t. At 0.6 T, the respective values are 89.0%, 90.8%, and 91.5%, compared with 87.7% for the control. At 0.8 T, the intermediate dosage leads with 84.7%, followed by 83.8% at 2400 g/t and 83.0% at 600 g/t. Thus, the highest dosage is not consistently the highest-yield treatment.

CC BY

REMUNOM
ISSN 2178-6925

Received: 10/11/2026 - **Accepted:** 15/11/2026
Vol: 13.24
DOI: 10.66104/x7btvw60
Pages: 1-29

Figure 6. Nonmagnetic mass recovery of bauxite versus magnetic flux density for the reagent-free control and sodium silicate (SS) at 600, 1200, and 2400 g/t. Error bars represent standard deviations (n = 3).



At 1.0 T, the recoveries remain separated: 75.6%, 78.1%, and 76.9% for 600, 1200, and 2400 g/t. At 1.2 T, all three curves reach 75.1% at the adopted reporting precision. This value exceeds the control by 4.7 percentage points, but the dosage distinction has disappeared. From 1.0 to 1.2 T, the lowest dosage loses only 0.5 percentage point, whereas the intermediate dosage loses 3.0 points. The convergence therefore arises from different responses over the final field interval, not from identical behavior throughout the experiment.

This result contrasts with the dispersion curve, where increasing SS dosage produces a sustained increase in suspended fraction. It suggests that a higher dispersion percentage does not necessarily preserve an advantage under stronger magnetic capture. One interpretation is that additional material remaining nonmagnetic at intermediate fields is captured when the field increases. Another is that the relevant particle associations differ from those controlling the sedimentation response. Product mineralogy would be needed to distinguish between capture of iron-bearing particles and capture of nonmagnetic material associated with them.

CC BY

REMUNOM
ISSN 2178-6925

Received: 10/11/2026 - **Accepted:** 15/11/2026
Vol: 13.24
DOI: 10.66104/x7btvw60
Pages: 1-29

Ma demonstrated that sodium silicate dispersion of kaolinite depends strongly on pH and dissolved cations: under controlled pH, a pronounced response occurred at pH 7, while calcium- and magnesium-induced coagulation was not effectively reversed. This is particularly pertinent to a separation conducted with tap water, whose ionic composition has not been quantified here. It provides a plausible reason for a limited SS response but does not prove that calcium or magnesium caused the observed convergence. Alexandrino and colleagues also investigated hematite dispersion and zeta potential, showing that the two measurements must be evaluated under specific reagent and pH conditions.

Silicate interaction with iron-bearing surfaces is independently supported by the spectroscopic investigation of Yang and colleagues on synthetic magnetite. Its relevance is evidence that silicate can interact with an iron oxide, not proof of the same surface species on the present hematite and goethite. Consequently, the SS behavior should be interpreted as the combined response of several mineral surfaces and the solution environment. Assigning the maximum-field convergence exclusively to insufficient kaolinite dispersion would overlook potential changes in iron-mineral association and capture.

3.5 Comparative assessment of chemical dispersants

The integrated comparison separates two questions: which reagent increases the operational dispersion index most strongly, and which treatment retains the greatest nonmagnetic mass at a specified field. SHMP exhibited the highest observed dispersion index across the tested dosage range, although the differences among reagents should be interpreted descriptively. The second has no field-independent answer. At 600 g/t and 0.6 T, the order is SHMP > SS > SMT; at 1200 g/t and the same field, SS and SMT exceed SHMP. At 1.2 T and 2400 g/t, SMT gives 79.8%, SHMP 79.2%, and SS 75.1%.

All reagents increase nonmagnetic mass recovery over the control at 1.2 T, but their dosage dependence differs. SHMP gives a progressive increase that becomes small between the two upper dosages. SMT has a larger step between 600 and 1200 g/t, followed by a smaller increment. SS gives no resolved dosage

CC BY

REMUNOM
ISSN 2178-6925

Received: 10/11/2026 - **Accepted:** 15/11/2026
Vol: 13.24
DOI: 10.66104/x7btvw60
Pages: 1-29

separation at that field. The effect is therefore an interaction between reagent identity, dosage, and magnetic conditions, not a single monotonic relationship between dispersion and yield. This description refers to the observed pattern and does not imply a fitted statistical interaction term.

A direct comparison of dispersion and separation is strongest at 600 and 1200 g/t, which occur in both experimental series. The 2400 g/t magnetic tests have no matching measured point in Figure 3, whose adjacent dispersion dosages are 2000 and 3000 g/t.

The physical interpretation must account for competing consequences of aggregate breakup. Detachment of weakly magnetic particles from nonmagnetic grains can facilitate their separation, while detachment of nonmagnetic fines from a captured iron-rich aggregate can increase nonmagnetic yield. Breakup of an aggregate composed mainly of weakly magnetic fines can decrease effective capture size. These mechanisms may operate simultaneously. Wang and Heiskanen documented mineral-dependent dispersion and sedimentation behavior in phosphate- and silicate-treated systems; Alvim and Fernandes Lima investigated selective flocculation before magnetic separation of ultrafine iron ore. These studies reinforce the distinction between dispersing all particles and arranging particle associations favorably for a particular separation objective.

The relationship between capture and particle size provides a conceptual explanation. In an idealized dilute system, magnetic force scales with particle volume, susceptibility contrast, and the field-gradient term, whereas viscous drag scales differently with particle size. An aggregate can therefore follow a different trajectory from its constituent grains, even when chemical conditioning leaves the intrinsic mineral susceptibilities unchanged. For a real bauxite pulp, aggregate composition, matrix interception, hydrodynamic transport, and entrainment complicate that balance. Without measured aggregate sizes and matrix conditions, this force argument explains possible trends but does not predict the observed recoveries quantitatively.

Water chemistry adds another source of conditional behavior. F. Rao and colleagues observed that kaolinite stability in aluminum salt solutions changed

CC BY

REMUNOM
ISSN 2178-6925

Received: 10/11/2026 - **Accepted:** 15/11/2026
Vol: 13.24
DOI: 10.66104/x7btvw60
Pages: 1-29

nonmonotonically with concentration. This shows why dissolved-ion effects cannot always be reduced to simple double-layer compression. Phosphate treatment may also alter the later adsorption environment: Choi and colleagues investigated collector adsorption on kaolinite in the presence of a long-chain phosphate. Such interactions matter if conditioned material enters another reagent stage, although no subsequent flotation operation is evaluated in the present experiment. A higher reagent dose may therefore have effects beyond the immediate recovery curve.

The practical implication is that a dispersion screening test narrows the choice of conditioning treatments but does not replace magnetic separation testing. The 1200 g/t treatments retain 78.7% with SHMP and 79.0% with SMT at 1.2 T, close to their respective 2400 g/t results. These observations identify intermediate dosage as an informative point for further assessment of product quality and reagent consumption. They do not establish an economic optimum. Likewise, the absence of a high-field SS dosage benefit argues against assuming that increased consumption will produce increased mass yield under those conditions.

Huang and colleagues provide a complementary example from diasporic bauxite: selective flocculation increased the alumina-to-silica mass ratio from 5.68 to 8.90 at 86.98% alumina recovery, using sodium carbonate and sodium polyacrylate at pH 9.5 to 10.0. That separation depended on different responses of aluminum minerals and silicates. Its quantitative performance is not a benchmark for the present gibbsitic material, but it illustrates the additional evidence needed to connect particle conditioning to a demonstrated beneficiation outcome.

Finally, the nonmagnetic stream contains an unresolved mixture of mineral phases. In the locked-cycle work reported by Kurusu and colleagues, magnetic separation increased available alumina from 29.7% to 52.6%, while the reported circuit mass yield decreased from 27.8% to 13.3%. That example demonstrates that a lower mass yield can accompany a higher product grade. The present study establishes that dispersants redistribute mass between separation products; determining whether that redistribution improves bauxite quality requires feed and product assays, alumina recovery, and iron rejection on a consistent mass-balance basis.

CC BY

REMUNOM
ISSN 2178-6925

Received: 10/11/2026 - **Accepted:** 15/11/2026
Vol: 13.24
DOI: 10.66104/x7btvw60
Pages: 1-29

4. Conclusions

The bauxite contains gibbsite, kaolinite, goethite, hematite, and anatase, providing a multiphase system in which chemical conditioning can affect both like-particle aggregation and associations between minerals. The size curve gives d_{80} of 73 μm and d_{90} of 112 μm. The electrokinetic response changes from +20.2 mV at pH 2 to −42.9 mV at pH 12, with small potential magnitudes near pH 8 to 9 and a sign change between pH 9 and 10.

SHMP produces the highest degree of dispersion at every nonzero dosage. At 3000 g/t, dispersion reaches 46%, compared with 41% for SMT, 38% for SS, and 18% without reagent. All three curves exhibit diminishing incremental gains at high dosage.

The dispersion ranking does not consistently predict nonmagnetic mass recovery. SHMP at 600 g/t gives 90.8% recovery at 0.6 T, exceeding SMT and SS at that dosage. At 1.2 T, 2400 g/t SMT gives 79.8%, compared with 79.2% for SHMP and 70.4% for the control. SS converges to 75.1% across the three tested dosages at 1.2 T. The small difference between the highest SHMP and SMT recoveries is descriptive and does not establish statistical superiority.

Chemical conditioning therefore changes bauxite mass partitioning in a manner dependent on dosage and field. Intermediate SHMP and SMT dosages approach the maximum-field yields obtained at twice their dosage, while increased SS dosage provides no resolved benefit at that field.

These results demonstrate changes in nonmagnetic mass recovery under the investigated conditions, but do not establish improvements in product quality, alumina recovery, or iron rejection. Chemical characterization of the separation products and component mass balances would be necessary to evaluate these outcomes.

CC BY

REMUNOM
ISSN 2178-6925

Received: 10/11/2026 - **Accepted:** 15/11/2026
Vol: 13.24
DOI: 10.66104/x7btvw60
Pages: 1-29

References

Alexandrino, Júnia Soares, et al. “Dispersion Degree and Zeta Potential of Hematite.” *Rem: Revista Escola de Minas*, vol. 69, no. 2, 2016, pp. 193–198, https://doi.org/10.1590/0370-44672014690073.

Alkan, Mahir, et al. “Electrokinetic Properties of Kaolinite in Mono- and Multivalent Electrolyte Solutions.” *Microporous and Mesoporous Materials*, vol. 83, no. 1–3, 2005, pp. 51–59, https://doi.org/10.1016/j.micromeso.2005.03.011.

Alvim, E. S., and R. M. Fernandes Lima. “Selective Flocculation/magnetic Separation of Ultrafine Iron Ore Particles with Corn Starch and Polyacrylamides: A Comparative Study.” *Mineral Processing and Extractive Metallurgy Review*, vol. 45, no. 6, 2024, pp. 606–615, https://doi.org/10.1080/08827508.2023.2214293.

Amorós, José Luis, et al. “Electrokinetic and Rheological Properties of Highly Concentrated Kaolin Dispersions: Influence of Particle Volume Fraction and Dispersant Concentration.” *Applied Clay Science*, vol. 49, no. 1–2, 2010, pp. 33–43, https://doi.org/10.1016/j.clay.2010.03.020.

Andreola, Fernanda, et al. “Release of Ions from Kaolinite Dispersed in Deflocculant Solutions.” *Applied Clay Science*, vol. 36, no. 4, 2007, pp. 271–278, https://doi.org/10.1016/j.clay.2006.10.002.

Andreola, Fernanda, et al. “Role of the Surface Treatment in the Deflocculation of Kaolinite.” *Journal of the American Ceramic Society*, vol. 89, no. 3, 2006, pp. 1107–1109, https://doi.org/10.1111/j.1551-2916.2005.00814.x.

Ashrafi, Amirhossein, et al. “An Investigation into the Pretreating of a Low-Grade Bauxite Ore Using Magnetic Separation and Flotation Processes.” *Rudarsko-geološko-naftni zbornik*, vol. 40, no. 3, 2025, pp. 119–130, https://doi.org/10.17794/rgn.2025.3.9.

Bass, Jonathan L., and Gary L. Turner. “Anion Distributions in Sodium Silicate Solutions. Characterization by ^{29}Si NMR and Infrared Spectroscopies, and Vapor Phase Osmometry.” *The Journal of Physical Chemistry B*, vol. 101, no. 50, 1997, pp. 10638–10644, https://doi.org/10.1021/jp9715282.

Batista e Silva, Gustavo Victor, et al. “Effect of Ultrasonic Pre-Treatment on the Reverse Flotation of Kaolinite from Bauxite.” *Mineral Processing and Extractive Metallurgy Review*, vol. 45, no. 8, 2024, pp. 982–990, https://doi.org/10.1080/08827508.2024.2351061.

Bolsaitis, P., et al. “Beneficiation of Ferruginous Bauxites by High-Gradient Magnetic Separation.” *International Journal of Mineral Processing*, vol. 8, no. 3, 1981, pp. 249–263, https://doi.org/10.1016/0301-7516(81)90015-6.

Castellini, Elena, et al. “Deflocculant Effects on the Surface Properties of Kaolinite Investigated Through Malachite Green Adsorption.” *Colloids and Surfaces A:*

CC BY

REMUNOM
ISSN 2178-6925

Received: 10/11/2026 - **Accepted:** 15/11/2026
Vol: 13.24
DOI: 10.66104/x7btvw60
Pages: 1-29

Physicochemical and Engineering Aspects, vol. 329, no. 1–2, 2008, pp. 31–37, https://doi.org/10.1016/j.colsurfa.2008.06.045.

Castellini, Elena, et al. “Sodium Hexametaphosphate Interaction with 2:1 Clay Minerals Illite and Montmorillonite.” *Applied Clay Science*, vol. 83-84, 2013, pp. 162–170, https://doi.org/10.1016/j.clay.2013.08.031.

Castellini, Elena, et al. “Thermodynamic Aspects of the Adsorption of Hexametaphosphate on Kaolinite.” *Journal of Colloid and Interface Science*, vol. 292, no. 2, 2005, pp. 322–329, https://doi.org/10.1016/j.jcis.2005.05.065.

Choi, I.-K., et al. “The Effect of a Long Chain Phosphate on the Adsorption of Collectors on Kaolinite.” *Minerals Engineering*, vol. 6, no. 11, 1993, pp. 1191–1197, https://doi.org/10.1016/0892-6875(93)90096-6.

Gonçalves, S. G., et al. “Efeito de aditivos no comportamento reológico do rejeito da bauxita.” *Cerâmica*, vol. 61, no. 357, 2015, pp. 1–5, https://doi.org/10.1590/0366-69132015613571808.

Han, Yonghua, et al. “Interactions Between Kaolinite Al–OH Surface and Sodium Hexametaphosphate.” *Applied Surface Science*, vol. 387, 2016, pp. 759–765, https://doi.org/10.1016/j.apsusc.2016.07.002.

Haselhuhn, Howard J. “Dispersant Adsorption and Effects on Settling Behavior of Iron Ore.” *Minerals & Metallurgical Processing*, vol. 30, no. 3, 2013, pp. 188–189, https://doi.org/10.1007/bf03402269.

Herrington, T. M., et al. “The Surface Charge of Kaolin.” *Colloids and Surfaces*, vol. 68, no. 3, 1992, pp. 161–169, https://doi.org/10.1016/0166-6622(92)80200-l.

Huang, Chuan-bing, et al. “Separation of Aluminosilicates and Diaspore from Diasporic-Bauxite by Selective Flocculation.” *Journal of Central South University of Technology*, vol. 15, no. 4, 2008, pp. 520–525, https://doi.org/10.1007/s11771-008-0098-4.

Johnson, Stephen B., et al. “Surface Chemistry–rheology Relationships in Concentrated Mineral Suspensions.” *International Journal of Mineral Processing*, vol. 58, no. 1–4, 2000, pp. 267–304, https://doi.org/10.1016/s0301-7516(99)00041-1.

Kasai, Eiki, et al. “Removal of Iron Minerals from Bauxite Ore by HGMS.” *Shigen-to-Sozai*, vol. 109, no. 10, 1993, pp. 817–822, https://doi.org/10.2473/shigentosozai.109.817.

Kumar, N., et al. “Probing the Surface Charge on the Basal Planes of Kaolinite Particles with High-Resolution Atomic Force Microscopy.” *Langmuir*, vol. 33, no. 50, 2017, pp. 14226–14237, https://doi.org/10.1021/acs.langmuir.7b03153.

CC BY

REMUNOM
ISSN 2178-6925

Received: 10/11/2026 - **Accepted:** 15/11/2026
Vol: 13.24
DOI: 10.66104/x7btvw60
Pages: 1-29

Kurusu, Renata Salles, et al. “Concentration of Bauxite Fines via Froth Flotation.” *Rem: Revista Escola de Minas*, vol. 62, no. 3, 2009, pp. 271–276, https://doi.org/10.1590/s0370-44672009000300003.

Liu, Caipeng, et al. “Effect of Sodium Hexametaphosphate on the Separation of Fine Quartz-Magnetite by Magnetic Separation: A Study of Dispersion Properties and Mechanism.” *Separation and Purification Technology*, vol. 359, 2025, article 130352, https://doi.org/10.1016/j.seppur.2024.130352.

Ma, Mark. “The Dispersive Effect of Sodium Silicate on Kaolinite Particles in Process Water: Implications for Iron-Ore Processing.” *Clays and Clay Minerals*, vol. 59, no. 3, 2011, pp. 233–239, https://doi.org/10.1346/ccmn.2011.0590302.

Miller, Jan D., et al. “Surface Characteristics of Kaolinite and Other Selected Two Layer Silicate Minerals.” *The Canadian Journal of Chemical Engineering*, vol. 85, no. 5, 2007, pp. 617–624, https://doi.org/10.1002/cjce.5450850508.

Missana, Tiziana, and Andrés Adell. “On the Applicability of DLVO Theory to the Prediction of Clay Colloids Stability.” *Journal of Colloid and Interface Science*, vol. 230, no. 1, 2000, pp. 150–156, https://doi.org/10.1006/jcis.2000.7003.

Quezada, Gonzalo R., et al. “Experimental and Simulation Studies on Hematite Interaction with Na-Metasilicate Pentahydrate.” *Molecules*, vol. 28, no. 8, 2023, article 3629, https://doi.org/10.3390/molecules28083629.

Rao, D. S., and B. Das. “Characterization and Beneficiation Studies of a Low Grade Bauxite Ore.” *Journal of The Institution of Engineers (India): Series D*, vol. 95, no. 2, 2014, pp. 81–93, https://doi.org/10.1007/s40033-014-0050-8.

Rao, Feng, et al. “Stability of Kaolinite Dispersions in the Presence of Sodium and Aluminum Ions.” *Applied Clay Science*, vol. 51, no. 1–2, 2011, pp. 38–42, https://doi.org/10.1016/j.clay.2010.10.023.

Rodrigues, Otávia Martins Silva, et al. “Kaolinite Removal from Bauxite by Flotation.” *REM - International Engineering Journal*, vol. 69, no. 3, 2016, pp. 349–353, https://doi.org/10.1590/0370-44672014690093.

Shao, Y., et al. “Wet High Intensity Magnetic Separation of Iron Minerals.” *Physical Separation in Science and Engineering*, vol. 8, no. 1, 1996, pp. 41–51, https://doi.org/10.1155/1996/34321.

Wang, Qun, and Kari Heiskanen. “Dispersion Selectivity and Heterocoagulation in Apatite-Hematite-Phlogopite Fine Particle Suspensions I. Dispersion of Single Minerals.” *International Journal of Mineral Processing*, vol. 35, no. 1–2, 1992, pp. 121–131, https://doi.org/10.1016/0301-7516(92)90008-k.

CC BY

REMUNOM
ISSN 2178-6925

Received: 10/11/2026 - **Accepted:** 15/11/2026
Vol: 13.24
DOI: 10.66104/x7btvw60
Pages: 1-29

Williams, D. J. A., and K. P. Williams. “Electrophoresis and Zeta Potential of Kaolinite.” *Journal of Colloid and Interface Science*, vol. 65, no. 1, 1978, pp. 79–87, https://doi.org/10.1016/0021-9797(78)90260-6.

Yang, Xiaofang, et al. “A Study of Sodium Silicate in Aqueous Solution and Sorbed by Synthetic Magnetite Using in Situ ATR-FTIR Spectroscopy.” *Journal of Colloid and Interface Science*, vol. 328, no. 1, 2008, pp. 41–47, https://doi.org/10.1016/j.jcis.2008.08.061.

CC BY